Imaging of oscillatory behavior in event-related MEG studies

Dimitrios Pantazis[a], Darren L. Weber[b], Corby C. Dale[b], Thomas E. Nichols [c], Gregory V. Simpson [b], Richard M. Leahy[a]

[a]Signal and Image Processing Institute, University of Southern California, Los Angeles, CA 90089-2564, USA
[b]Dynamic Neuroimaging Laboratory, Department of Radiology, University of California San Francisco, San Francisco, CA 94143, USA
[c]Department of Biostatistics, University of Michigan, Ann Arbor, MI 48109-2029, USA

ABSTRACT

Since event-related components in MEG (magnetoencephalography) studies are often buried in background brain activity and environmental and sensor noise, it is a standard technique for noise reduction to average over multiple stimulus-locked responses or "epochs". However this also removes event-related changes in oscillatory activity that are not phase locked to the stimulus. To overcome this problem, we combine time-frequency analysis of individual epochs with cortically-constrained imaging to produce dynamic images of brain activity on the cerebral cortex in multiple time-frequency bands. While the SNR in individual epochs is too low to see any but the strongest components, we average signal power across epochs to find event related components on the cerebral cortex in each frequency band. To determine which of these components are statistically significant within an individual subject, we threshold the cortical images to control for false positives. This involves testing thousands of hypotheses (one per surface element and time-frequency band) for significant experimental effects. To control the number of false positives over all tests, we must therefore apply multiplicity adjustments by controlling the familywise error rate, i.e. the probability of one or more false positive detections across the entire cortex. Applying this test to each frequency band produces a set of cortical images showing significant event-related activity in each band of interest. We demonstrate this method in applications to high density MEG studies of visual attention.

Keywords: Event-related MEG studies, time-frequency analysis, Morlet wavelets, permutation tests, familywise error rate

1. INTRODUCTION

Event-related changes in oscillatory brain activity have been widely observed in response to sensory stimuli, and during motor and cognitive tasks, in a variety of human EEG and MEG experiments. [1–5] These changes often localize in specific brain areas and frequency bands, depending on the underlying neuronal processes. Increases and descreases in oscillatory power, relative to some baseline, can be attributed to event-related synchronization and desynchronization of neuronal populations.[6,7]

Task-related activity that is precisely phase locked to the stimulus is referred to as an evoked response and averaging of such respones over multiple epochs will result in increased signal to noise ratio relative to background noise and brain activity unrelated to the task, as illustrated in Fig. 1. However, there are other oscillatory components in EEG and MEG data whose power is modulated in response to a task or stimulus but which are not phase locked to the stimulus. Averaging of these non-phase locked components over multiple epochs will result in signal cancellation as also illustrated in Fig. 1. These induced components in the data are believed to play an important role in neural communication. Consequently producing spatial maps of these induced oscillatory changes is important for developing an increased understanding of communication in the brain.

Since event-related components in MEG studies are often lost in background brain activity and environmental and sensor noise, it is a standard technique for noise reduction to average over stimulus-locked responses. However this also removes induced oscillatory changes in brain activity, because they are not phase locked to the stimulus (Fig. 1). To

Corresponding Author: Richard M. Leahy, E-mail: leahy@usc.edu, Telephone: 1 213 740 4659.

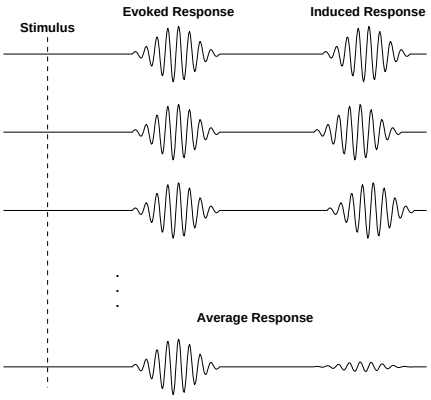

Figure 1. MEG brain activity in response to a task or stimulus consists of evoked components that are phase-locked to the stimulus and induced components that are not. While averaging over epochs enhances the phase locked SNR, averaging also results in suppresion of the non-phase locked components.

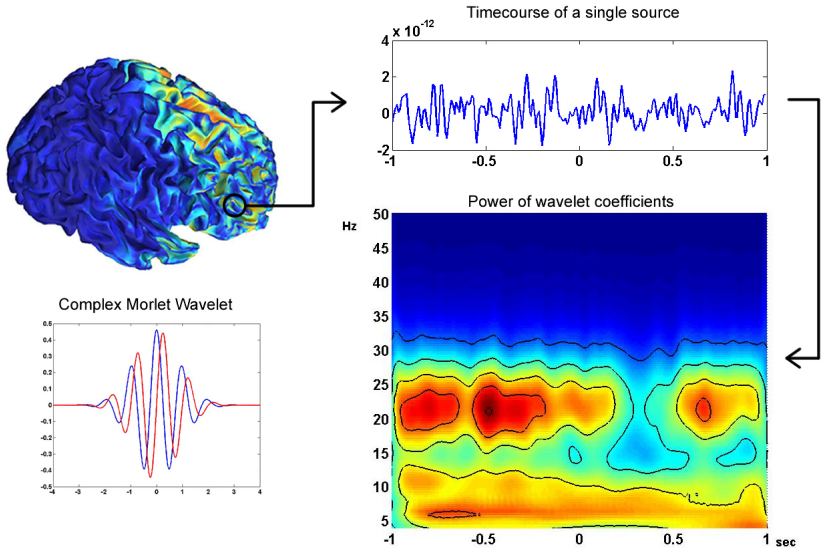

Figure 2. Time-varying frequency components of a source on the frontal lobe, after averaging over many epochs; we notice desynchronization in the β band 250-600ms after stimulus. The Morlet wavelet is a Gaussian-windowed complex sinusoid with the real part shown in blue, and the imaginary part in red.

overcome the problem of cancellation of non-phase locked oscillatory components, we use time-frequency analysis [8,9] of each individual epoch and then analyze event-related changes by computing average power across epochs in time-frequency space. Figure 2 illustrates time-frequency analysis using Morlet wavelets [10] for a single source on the frontal lobe in an MEG study involving attention to a visual task. Repeating this procedure at all cortical locations, we can produce dynamic cortical images in multiple frequency bands. While the SNR in individual epochs is too low to see any but the strongest components, averaging signal power across epochs should reveal significant event-related activity across the entire time-frequency space.

Objective assessment of the above cortical images requires a principled approach to identifying regions of activity in frequency bands. This analysis involves testing thousands of hypotheses (one per surface element and time-frequency band) for statistically significant experimental effects. This raises the possibility of large numbers of false positives simply as a result of multiple hypothesis testing. To control the number of false positives over all tests we must therefore consider the multiple hypothesis testing problem. The standard approach, and the one investigated in this paper, is to control the Familywise Error Rate (FWER), i.e. the chance of one or more false positives under the null hypothesis. Methods

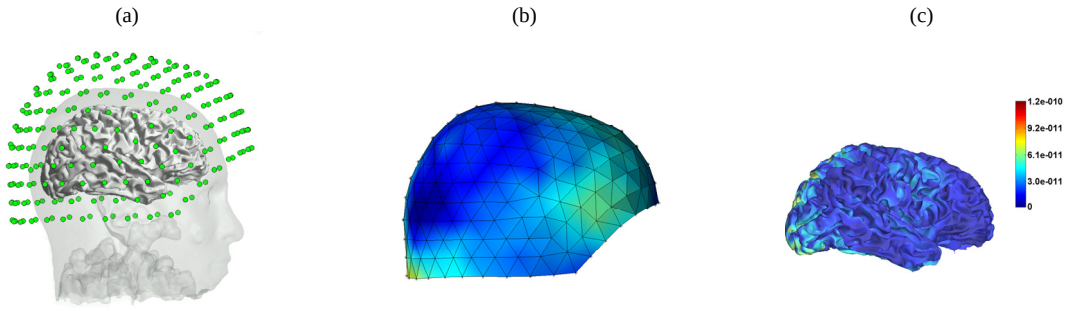

Figure 3. MEG model; (a) Sensor arrangement of a 275-channel CTF MEG system, (b) Topography of sensor measurements M_{itj}, (c) Min-norm inverse solution X_{itj} on a tessellated cortical surface

that control the FWER, and consider the spatial dependence of the data, make inferences based on the global maximum distribution of the image statistics over space and frequency bands. The maximum distribution can be estimated either parametrically (random field theory) or non-parametrically (permutation tests).

Recently, there have been many studies investigating oscillatory components and their relation to cognitive, motor and sensory tasks.[11–13] Time-frequency analysis has been successfully used to detect and localize evoked and induced responses.[8, 14, 15] At the same time, non-parametric permutation tests are widely used in statistical processing of neuroimaging data.[6, 16–18] In this paper we combine time-frequency analysis of individual epochs with minimum norm imaging to produce dynamic cortical images in multiple frequency bands. We then average signal power across epochs to find event related components in each band. To detect statistically significant differences between two conditions, such as post-stimulus vs. baseline, we use a permutation test. Applying this test to each frequency band produces a set of cortical images showing significant event-related activity in each band of interest. We demonstrate this method in application to high density MEG studies of visual attention.

2. METHOD

Our goal is to detect spatial regions of activity in MEG-based cortical maps in specific time-frequency bands, while controlling the FWER. The methods we describe below also apply directly to cortical maps computed from EEG data, since the inverse imaging methods differ only in the forms of their lead field matrices. [19] Although for convenience we describe them in the context of baseline vs. post-stimulus comparison, these can be used to compare any two conditions. In this section we first describe our MEG data model. We then present a method based on non-parametric permutation tests for controlling the FWER in time-frequency maps in MEG experiments.

2.1. Model

We assume that MEG data are collected as a set of J stimulus-locked event-related epochs (one per stimulus repetition), each consisting of a pre- and post-stimulus interval. Each epoch consists of an array of data M ($n_{\text{channels}} \times n_{\text{timepoints}}$) representing the measured magnetic field at each sensor as a function of time. The measurements M are linearly related with the brain activation X ($n_{\text{sources}} \times n_{\text{timepoints}}$) as:

$$M = GX + N \tag{1}$$

where G ($n_{\text{channels}} \times n_{\text{sources}}$) is the forward operator and N represents additive noise in the channel measurements. The lead field matrix G depends on the shape and conductivity of the head and can be computed using a simplified spherical head model, or more accurately, using boundary or finite element methods that account for the true shape and conductivity within the head.[19, 20]

A cortical map can be computed for each epoch by applying a Tikhonov regularized minimum norm inverse method to produce an estimate of the temporal activity at each surface element in the cortex (Fig. 3):

$$X = (G^T G + \lambda I)^{-1} G^T M \tag{2}$$

We write the reconstructed cortical maps as $\{X_{itj}\}$, where $i = 1, \ldots, S$, $t = -N_0 + 1, \ldots, N$, and $j = 1, \ldots, J$ are indices in space, time, and epoch, respectively. We let $t = 1$ correspond to the stimulus event time so that there are N_0 pre-stimulus time points. We use the pre-stim data to estimate the baseline mean m_{ij} and standard deviation s_{ij} at each spatial element i at epoch j, by averaging over time t. We then estimate the noise-normalized centered data as:

$$Y_{itj} = \frac{X_{itj} - m_{ij}}{s_{ij}} \tag{3}$$

2.2. Wavelet Expansion

We use a continuous wavelet transform[9] to decompose the source timeseries ($Y_{itj}, t = -N_0+1, \ldots, N$) into their wavelet coefficients. Unlike the Fourier transform, which decomposes a signal into infinite length sines and cosines and loses all time localization information, the continuous wavelet transform basis functions are scaled and shifted versions of the time-localized mother wavelet. A commonly used continuous time wavelet is the complex Morlet wavelet, [10] a Gaussian-windowed complex sinusoid defined as:

$$w_{tf} = (\pi b)^{-0.5} e^{2i\pi ft} e^{-t^2/b} \tag{4}$$

where b is the bandwidth parameter.

For each epoch j and each source i we obtain an estimate of the time-varying frequency components by expanding the timeseries using Morlet wavelets as:

$$C_{itfj} = Y_{itj} \star w_{tf} \tag{5}$$

where ($\star$) denotes the convolution operator over the time index t, and C_{itfj} are the complex wavelet coefficients. Because the wavelet decomposition is linear and computed entirely in the time domain, while the inverse operator (2) is computed entirely in the spatial domain, the two operators commute. In practice it is more computationally efficient to first compute the wavelet decomposition in the channel domain, and then to apply the inverse operator (2) to each of the wavelet coefficients.

2.3. Statistics

Our goal is to detect spatial regions of activity in MEG-based cortical maps that exhibit task-related changes in oscillatory behavior. Based on our understanding of neuronal processes related to visual and sensorimotor tasks, we define time-frequency bands $S_k = \{(t, f), t \in [t_0^k\ t_1^k], f \in [f_0^k\ f_1^k]\}$, that may contain significant event-related components of brain activity. For example, in Fig. 5 we chose a total of 12 time-frequency bands corresponding to early (200-500ms) and late (700-1000ms) responses in the θ (4-7Hz), α low (8-10Hz), α high (11-14Hz), β low (14-19Hz), β high (20-30Hz), and γ (30-50Hz) frequency regions. As described below, we also select corresponding time-frequency bands in the prestimulus interval against which to test for event related changes. We estimate the total power in these bands by integrating over time and frequency:

$$E_{ikj} = \iint_{(t,f)\in S_k} |C_{itfj}|^2 \text{dtdf} \tag{6}$$

We take the standard massively univariate approach and model each spatial location seperately. [21] For each spatial location, the model then amounts to a one-way ANOVA model with repeated measures:

$$E_{ikj} = \mu_{ik} + \epsilon_{ikj} \tag{7}$$

Our goal is to identify, in each band, those cortical areas where there are significant pre- and post-stimulus energy differences. Using the notation k^+ for a post-stimulus time period $t \in [t_0^k\ t_1^k]$, and k^- for a pre-stimulus period $t \in [-t_1^k\ -t_0^k]$, we test the hypothesis:

$$H_0 : \mu_{ik^+} = \mu_{ik^-} \tag{8}$$

for all source locations and time-frequency bands.

We use the standard statistic for pairwise testing:

$$T_{ik} = \frac{\overline{E}_{ik^+\cdot} - \overline{E}_{ik^-\cdot}}{\sigma_{ik}} \tag{9}$$

where the bar indicates an average over the dotted subscript. We assume a heteroscedastic model, i.e. we allow different distributions for residuals ϵ_{ikj} occurring for different source locations i and time-frequency bands k. Then, the variance σ^2_{ik} is estimated using the repeated measurements over the J epochs as:

$$\sigma_{ik} = \sqrt{\frac{\text{var}\{E_{ik^+j}\} + \text{var}\{E_{ik^-j}\}}{J}}\ , \quad \text{var}\{E_{ik^+j}\} = \sum_j \frac{(E_{ik^+j} - \overline{E}_{ik^+\cdot})^2}{J-1}\ , \quad \text{var}\{E_{ik^-j}\} = \sum_j \frac{(E_{ik^-j} - \overline{E}_{ik^-\cdot})^2}{J-1} \tag{10}$$

If the error terms ϵ_{ikj} in Eq. 7 follow a Gaussian distribution, the statistic T_{ik} follows a t-distribution with approximately ν_{ik} degrees of freedom, computed using the Satterthwaite method as [22]:

$$\nu_{ik} = (J-1)\frac{(\text{var}\{E_{ik^+j}\} + \text{var}\{E_{ik^-j}\})^2}{\text{var}^2\{E_{ik^+j}\} + \text{var}^2\{E_{ik^-j}\}} \tag{11}$$

Under the central limit theorem, this statement is approximately true even if the Gaussian assumption is violated provided the number of epochs J is large.

2.4. Multiplicity Adjustments

The massively univariate approach, as modeled in Eq. (7), involves testing thousands of hypotheses (one per surface element and time-frequency band) for statistically significant experimental effects. To effectively control the number of false positives over all tests we must therefore apply multiplicity adjustments by controlling the FWER. The FWER is directly related to the maximum statistic; one or more statistics T_{ik} will exceed the threshold u under the null hypothesis H_0 if and only if the maximum exceeds the threshold [*]:

$$\begin{aligned} P(\text{FWER}) &= P(\cup_{ik}\{|T_{ik}| > u\}|H_o) \\ &= P(\max_{ik}|T_{ik}| > u|H_o) \\ &= 1 - F_{\max|T|\ |H_o}(u) \\ &= 1 - (1-\alpha) = \alpha \end{aligned} \tag{12}$$

We use the absolute value because negative values of T_{ik} can also indicate significant changes in oscillatory power, and we therefore need a two-tailed test statistic. As shown in Eq. 12, we can control the FWER if we choose the threshold u to be in the $(1-\alpha)100^{th}$ percentile of the maximum distribution.

2.5. Permutation Tests

The multiplicity adjustments require the distribution of $\max_{ik}|T_{ik}|$. Even though we know each T_{ik} follows a t-distribution with ν_{ik} degrees of freedom (Subsection 2.3), it is impossible to evaluate analytically the maximum distribution; ν_{ik} varies over i and k, and the correlation structure among T_{ik} is unknown. Further, the distribution of E_{ikj} may deviate from Gaussian, and thus the distribution of T_{ik} may deviate from the t-distribution. While the effects of deviations from Gaussianity can be serious in univariate situations, the effects tend to be amplified in multiple testing applications where maximal statistics are considered.[23]

To overcome these problems, we use a non-parametric permutation method to estimate the distibution of $\widetilde{T}_{\cdot\cdot} = \max_{ik}|T_{ik}|$, where the tilde indicates a maximum over the dotted subscript. The standard approach to permutation tests is to find units exchangeable under the null hypothesis. Under the null hypothesis that there are no task-related differences between corresponding pre- and post-stimulus time-frequency bands, we can permute the energy in time-frequency bands E_{ik^+j} and E_{ik^-j}. The permutations can be applied over epochs, which are typically regarded as independent, but not over source locations and time-frequency bands, because we may destroy possible correlations in the data. Given J original epochs of MEG measurements, we have J repetitions of E_{ik^+j} and E_{ik^-j}. By randomly interchanging or permuting the pre- and post-stimulus time-frequency bands, we can create $M \leq \binom{2J}{J}$ permutation samples $E^*_{ik^+j}$ and $E^*_{ik^-j}$. The symbol (*) indicates that the statistics are created by permutation.

[*] F_X denotes the cumulative density function (CDF) of the random variable X

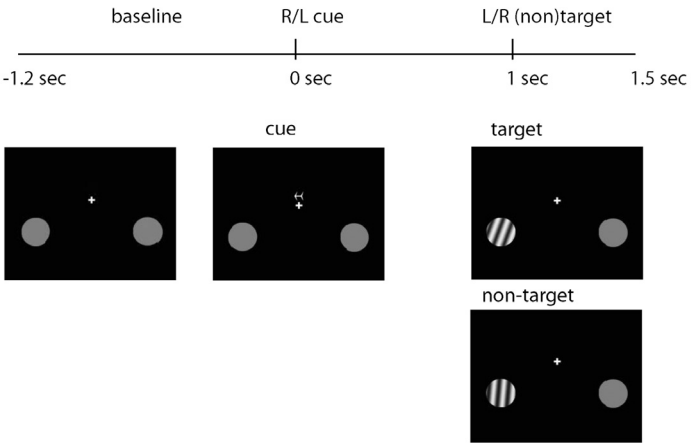

Figure 4. Illustration of the MEG visual attention study: Each trial presents a central arrow cue that directs attention to the lower left or right visual field, in anticipation of a second stimulus (S2), delivered 1 sec later on the left or right. The locations of the upcoming S2 are continuously marked by gray patches, to guide allocation of covert visual spatial attention. If the S2 (a B/W grating) occurs on the cued (attended) side, then subjects respond if it has the target orientation.

By applying Eq. 9 to the permuted data, we create permutation samples of T_{ik}:

$$T^*_{ik} = \frac{\overline{E}^*_{ik^+\cdot} - \overline{E}^*_{ik^-\cdot}}{\sigma^*_{ik}} \tag{13}$$

To obtain thresholds that control the FWER over space and time-frequency bands, we compute the permutation distribution of the maximum statistic:

$$\widetilde{T}^*_{\cdot\cdot} = \max_{ik} |T^*_{ik}| \tag{14}$$

We use this distribution to define a level α threshold: $\hat{F}^{-1}_{\widetilde{T}_{\cdot\cdot}}(1-\alpha)$. A band k has statistically significant energy at source i if T_{ik} (the original statistic) exceeds this threshold.

3. RESULTS

We illustrate this method using a high density MEG study of visual attention which produces activity in many different cortical regions forming functional networks. Following a 1.2 sec baseline period, a brief central arrow cue directs covert attention to the lower left or right visual field, in anticipation of a second stimulus (S2), delivered 1 sec later on the left or right (Fig. 4). The upcoming S2 consists of gratings slanted clockwise from the vertical by either 5 (non-target) or 20 (target) degrees, with a response required if the grating appears at the cued (attended) location (50%) and had the target orientation.

The MEG measurements were recorded using a whole-head CTF Omega system with 275 axial gradiometers. Horizontal and vertical EOGs were recorded and used to eliminate trials with eye movements or blinks. Data were collected using a bandpass filter of 0.3 to 200Hz at a 1.2kHz sampling rate, with trials defined off-line around stimulus events, and rejected for predefined anomalies in EEG or MEG signals. Anatomical data was acquired with a Philips 1.5 Tesla MRI scanner, using a SENSE head coil; T1 contrast was acquired in 200 axial slices (1.0x1.0x1.2 mm, TI/TE/TR/flip angle = 769.6 msec/3.7 msec/7.9 msec/8 degrees). A cortical surface was extracted from the MRI scan using BrainSuite, a brain surface extraction tool,[24] and coregistered to the MEG sensor arrangement. The MEG forward model was calculated based on an overlapping spheres model[25] using BrainStorm,[26] a Matlab toolbox for EEG&MEG data processing.

We applied our methodology to identify statistically significant differences between pre-cue baseline activity vs. post-cue responses. The MEG recordings consisted of $J = 276$ epochs, and were mapped onto the cortical surface using min-norm imaging and time-frequency analysis based on complex Morlet wavelets. We chose 12 bands to detect early

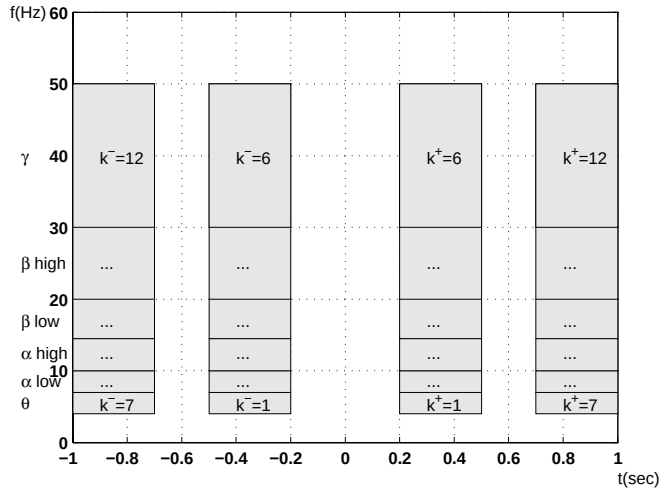

Figure 5. We tested 12 post-stimulus time-frequency bands against their baseline counterparts. All bands were 200-500ms or 700-1000ms after the presentation of the cue, in frequency regions: θ (4-7Hz), α low (8-10Hz), α high (11-14Hz), β low (14-19Hz), β high (20-30Hz), and γ (30-50Hz).

(200-500ms) and late (700-1000ms) post-cue stimulus responses, in θ (4-7Hz), α low (8-10Hz), α high (11-14Hz), β low (14-19Hz), β high (20-30Hz), and γ (30-50Hz) frequency regions. To detect changes from the baseline we also computed power in the corresponding prestimulus bands. We used Eqs. (9) and (13) to form t-statistics T_{ik}, from our original data, and T^*_{ik}, from $M = 1000$ permutation samples. Using the permutation distribution of $\max_{ik} |T^*_{ik}|$, we estimated the threshold $\hat{F}^{-1}_{\widetilde{T}_{..}}(1-\alpha) = 0.2628$ that controls the FWER at the $\alpha = 0.05$ level (Fig. 6).

Figure 7a shows example image maps from one subject of T_{ik}, for the θ and γ frequency bands at 700-1000ms after the presentation of a right cue ($k = 7$ and $k = 12$ respectively, in Fig. 5). Figure 7b shows thesholded versions of the same maps based on our permutation test.

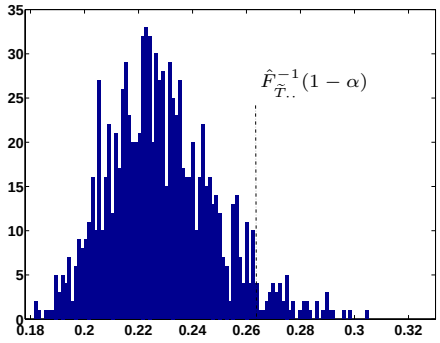

Figure 6. Empirical distribution $\hat{F}_{\widetilde{T}_{..}}$ of $\max_{ik} |T^*_{ik}|$.We use this distribution to estimate a threshold $\hat{F}^{-1}_{\widetilde{T}_{..}}(1-\alpha) = 0.2628$ that controls the FWER at the $\alpha = 0.05$ level.

The statistically thresholded images indicate gamma activity in multiple visual sensory areas with weak activity in the intra-parietal sulcus (IPS) and temporal parietal junction (TPJ). This pattern is consistent with models of parietal and sensory networks for visuospatial attention and supports a role for gamma in amplifying and maintaining a network of internal representations of the upcoming target stimulus. Significant increases in theta activity are seen in many of the same visual sensory and parietal areas. In addition, there are two non-corresponding areas that suggest an interesting functional dissociation between gamma and theta. The superior frontal gyrus and higher order visual areas such as inferior temporal lobe (indicated by arrows), have increased theta, but little or no gamma activity (see arrows). These areas are thought to be

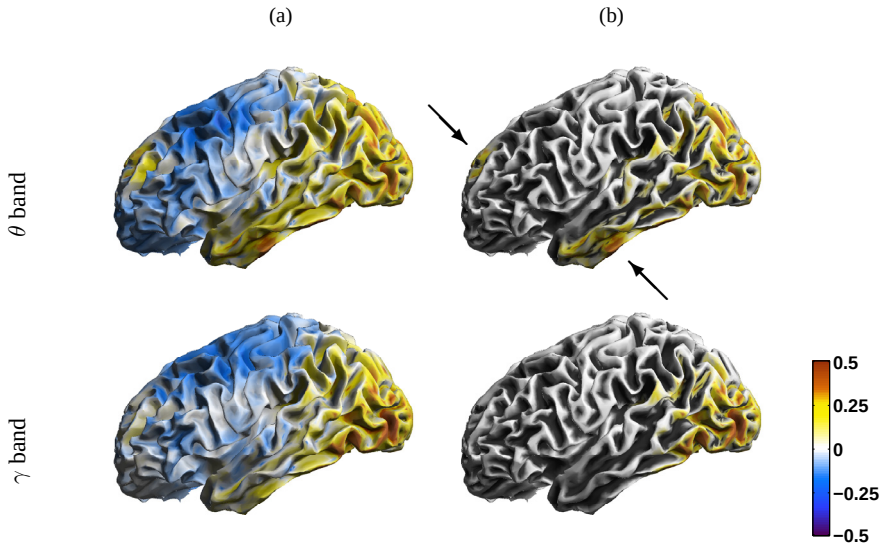

Figure 7. Normalized power difference maps of baseline vs. right cue for the visual-attention MEG study: (a) Unthresholded maps of T_{ik}, (b) Thresholded maps of T_{ik}, based on our permutation test. We used the threshold $\hat{F}^{-1}_{\tilde{T}_{\cdot\cdot}}(1-\alpha) = 0.2628$ to control the FWER at $\alpha = 0.05$ level. The colormap encodes percentage increase in energy in units of standard deviation. The thesholded maps reveal increased activity in the superior frontal gyrus and inferior temporal lobe (arrows), that are only significant in the θ band. These results suggest a functional dissociation between θ and γ bands.

involved in working memory and the cortical pattern suggests that theta plays a role in maintaining a representation of the anticipated target features, consistent with our findings in monkey recordings. [7] These preliminary findings are consistent with the hypothesis that there are overlapping yet distinct brain networks operating with different physiological processes to deploy and hold anticipatory attention.

4. CONCLUSION

In this paper we combined time-frequency analysis of individual epochs with minimum norm imaging to produce dynamic cortical images in multiple frequency bands. We then averaged signal power across epochs to find event related components in each band. To detect statistically significant differences between two conditions, such as post-stimulus vs. baseline, we used a permutation test. Applying this test to each frequency band produced a set of cortical images showing significant event-related activity in each band of interest. We demonstrated this method in application to high density MEG studies of visual attention. This ability to image statistically significant changes in brain oscillatory activity within individual subjects has a wide range of applications in basic cognitive neuroscience research and clinical studies.

ACKNOWLEDGMENTS

This work was supported in part by grants from NIBIB (R01 EB002010), NCRR (P41 RR013642), and NINDS (NS27900 and NS45171). We thank Cathy and Nick for MRI scanning, and Morgan Hough and Anne Findlay for technical support of MEG

REFERENCES

1. M. S. Worden, J. J. Foxe, N. Wang, and G. V. Simpson, "Anticipatory biasing of visuospatial attention indexed by retinotopically specific alpha-band EEG increases over occipital cortex," *Neuroscience* **20**(6), p. RC63, 1946.
2. K. Singh, G. R. Barnes, A. Hillebrand, E. M. Forde, and A. L. Williams, "Task-related changes in cortical synchronization are spatially coincident with the hemodynamic response," *Neuroimage* **1**(16), pp. 103–114, 2002.
3. G. Pfurtscheller and F. H. L. da Silva, "Event-related EEG/MEG synchronization and desynchronization: basic principles," in *Proceedings of the 11th International Conference on Biomagnetism*, T. U. Press, ed., **11**(110), pp. 1842–1857, 1999.

4. K. Jerbi, S. Baillet, J.-P. Lachaux, D. Pantazis, R. M. Leahy, and L. Garnero, "Modulations of power and synchronization of neural activity during sustained visuomotor coordination: An MEG study," in *The organization of Human Brain Mapping, 11th annual meeting*, June 2005.
5. E. Basar, C. Basar-Eroglu, S. Karakas, and M. Schurmann, "Gamma, alpha, delta, and theta oscillations govern cognitive processes," *Int. J. Psychophysiol.* **2-3**(39), pp. 241–248, 2001.
6. K. Singh, G. R. Barnes, and A. Hillebrand, "Group imaging of task-related changes in cortical synchronization using nonparametric permutation testing," *Neuroimage* **19**, pp. 1589–1601, 2003.
7. H. Lee, G. V. Simpson, N. K. Logothetis, and G. Rainer, "Phase locking of single neuron activity to theta oscillations during working memory in monkey," *Neuron* **45**, pp. 147–156, 2005.
8. N. H. Morgan and A. S. Gevins, "Wigner distributions of human event-related brain potentials," *IEEE Trans. BME* **33**, pp. 63–70, 1986.
9. J. K. Martin Vetterli, ed., *Wavelets and Subband Coding*, Prentice Hall PTR; 1st edition, April 1995.
10. A. Teolis, ed., *Computational Signal Processing With Wavelets (Applied and Numerical Harmonic Analysis)*, Birkhauser Boston, March 1998.
11. K. Jerbi, J.-P. Lachaux, S. Baillet, and L. Garnero, "Imaging cortical oscillations during sustained visuomotor coordination in MEG," in *Proceedings of ISBI 2004, Arlington, VA, USA*, April 2004.
12. R. Hari and R. Salmelin, "Human cortical oscillations: a neuromagnetic view through the skull," *Trends in Neurosciences* **20**, pp. 44–49, 1997.
13. C. Tallon-Baudry, O. Bertrand, C. Delpuech, and J. Permier, "Oscillatory gamma-band (30-70 Hz) activity induced by a visual search task in humans," *Neuroscience* **17**, pp. 722–734, January 1997.
14. O. Bertrand, C. Tallon-Baudry, and J. Pernier, "Time-frequency analysis of oscillatory gamma-band activity: wavelet approach and phase-locking estimation," in *Advances in Biomagnetism Research: Biomag96*, A. C, O. Y, S. G, S. S, and W. C, eds., *Springer-Verlag, New York*, 2000.
15. C. Tallon-Baudry, O. Bertrand, C. Delpuech, and J. Permier, "Stimulus specificity of phase-locked and non-phase-locked 40Hz visual responses in human," *Neuroscience* **16**(16), pp. 4240–4249, 1996.
16. D. Pantazis, T. E. Nichols, S. Baillet, and R. M. Leahy, "Spatiotemporal localization of significant activation in MEG using permutation tests," in *Proc. 18th Conf. Information Processing in Medical Imaging*, C. Taylor and J. A. Noble, eds., pp. 512–523, July 2003.
17. D. Pantazis, T. E. Nichols, S. Baillet, and R. M. Leahy, "A comparison of random field theory and permutation methods for the statistical analysis of MEG data," *Neuroimage (in press)* , 2004.
18. T. E. Nichols and A. P. Holmes, "Nonparametric permutation tests for functional neuroimaging: A primer with examples," *Human Brain Mapping* **15**, pp. 1–25, 2001.
19. S. Baillet, J. C. Mosher, and R. M. Leahy, "Electromagnetic brain mapping," *IEEE Signal Processins Magazine* **18**, pp. 14–30, 2001.
20. J. C. Mosher, R. M. Leahy, and P. S. Lewis, "EEG and MEG: Forward solutions for inverse problems," *IEEE Transactions of Biomedical Engineering* **46 (3)**, pp. 245–259, 1999.
21. K. J. Friston, A. P. Holmes, K. J. Worsley, J. B. Poline, C. Frith, and R. S. J. Frackowiak, "Statistical parametric maps in functional imaging: A general linear approach," *Human Brain Mapping* **2**, pp. 189–210, 1995.
22. F. E. Satterthwaite, "An approximate distribution of estimates of variance components," *Biometrics Bulletine* **2**, pp. 110–114, 1946.
23. P. H. Westfall and S. S. Young, eds., *Resampling Based Multiple Testing: Examples and Methods for p-Value Adjustment*, Wiley-Interscience, December 1992.
24. D. Shattuck and R. Leahy, "Brainsuite: An automated cortical surface identification tool," *Medical Image Analysis* **6**, pp. 129–142, June 2002.
25. M. Huang, J. Mosher, and R. Leahy, "A sensor-weighted overlapping-sphere head model and exhaustive head model comparison for MEG," *Phys. Med. Biol.* **44**, pp. 423–440, 1999.
26. S. Baillet, J. Mosher, and R. Leahy, "Brainstorm: A non-commercial matlab toolbox for MEG-EEG data visualization and processing," *http://neuroimage.usc.edu/brainstorm* , 2004.